INFRARED INSIGHT INTO THE NETWORK OF HYDROGENATED AMORPHOUS AND POLYCRYSTALLINE SILICON THIN FILMS

J. Müllerová

Department of Engineering Fundamentals, Faculty of Electrical Engineering, University of Žilina
Workplace Liptovský Mikuláš, ul. kpt. J. Nálepku 1390, 031 01 Liptovský Mikuláš, Slovakia
e-mail:mullerova@lm.utc.sk

Summary IR measurements were carried out on both amorphous and polycrystalline silicon samples deposited by PECVD on glass substrate. The transition from amorphous to polycrystalline phase was achieved by increasing dilution of silane plasma at the deposition process. The samples were found to be mixed phase materials. Commonly, infrared spectra of hydrogenated silicon thin films yield information about microstructure, hydrogen content and hydrogen bonding to silicon. In this paper, additional understanding was retrieved from infrared response. Applying standard optical laws, effective media theory and Clausius-Mossoti approach concerning the Si-Si and Si-H bonds under IR irradiation as individual oscillators, refractive indices in the long wavelength limit, crystalline, amorphous and voids volume fractions and the mass density of the films were determined. The mass density was found to decrease with increasing crystalline volume fraction, which can be attributed to the void-dominated mechanism of network formation.

1. INTRODUCTION

A wide range of characterization methods is commonly used in order to achieve a comprehensive overview of properties of silicon thin films deposited by plasma-enhanced chemical vapour deposition (PECVD). Hydrogenated amorphous silicon (a-Si:H) and polycrystalline silicon (poly-Si) enter numerous applications especially in thin-film photovoltaics. The structure and microstructure of the film feels the deposition conditions, substrate material and film thickness. Additional hydrogen in PECVD deposition favours the crystallisation due to the chemical rearrangement of a-Si:H network.

This work reports on experimental studies of the of a-Si:H and poly-Si thin films deposited by PECVD from hydrogen diluted silane. Infrared (IR) absorption measurements offer considerable knowledge about the role of hydrogen in the network of a-Si:H and poly-Si. The results are sensitive to the parameters of the deposition process. This is valid especially for amorphous materials. Therefore IR study can be applied to control the deposition conditions and to tailor the film properties for specific purposes, such as thin film applications in photovoltaics, optoelectronics, microelectronics etc., where the understanding, improvement and reproducibility of film properties facilitates mass production.

2. EXPERIMENTAL

Undoped Si:H thin films of the approximately same thickness ~ 400 nm were deposited at the Delft University of Technology, the Netherlands, on clean Corning 1737 glass substrates by 13.5 MHz rf excited parallel plate PECVD industrial deposition system (rf power 13.5 W) especially for extensive studies of photodegradation [1]. The deposition was performed at substrate temperature 194 °C and the total chamber pressure 200 Pa from hydrogen (H_2) to silane (SiH_4) plasma under varied H_2/SiH_4 gas flow (the dilution D).

The growth parameters of the samples are summarized in Table 1. Early knowledge of the growth-related structure, microstructure and optical properties was published elsewhere [2, 3]. X-ray diffraction and Raman scattering evidenced the progressive formation of crystalline Si with increasing D. Crystalline part fraction determined from Raman spectra and the hydrogen content c_H in atomic percent collected from IR spectra are in Table 1. According to this knowledge, samples # 0 – # 2 remained in the amorphous regime. At the dilution between 20 and 30 the transition between amorphous and crystalline phase occurred. At higher dilutions, the samples became a mixture of polycrystalline silicon with nano-sized grains and grain boundaries composed of amorphous Si and voids with decreasing hydrogen and post-deposition oxygen contamination [2, 3].

Tab. 1. Growth and growth-related parameters of the samples. Degree of crystallinity determined from Raman spectra, hydrogen content c_H from IR absorbance [2].

Sample	Dilution	Thickness [μm]	Degree of crystallinity [%]	c_H [at. %]
# 0	0	0.390	-	17.5
# 1	10	0.394	-	10.8
# 2	20	0.385	-	11.3
# 3	30	0.388	61	2.2
# 4	40	0.402	73	3.3
# 5	50	0.397	82	1.5

3. INFRARED ABSORPTION

The infrared absorption bands identify specific molecular bonds and enable to monitor the film composition and the microstructure of the compounds. In this study, FTIR-DIGILAB FTS 3000MX Excalibur spectrophotometer with the wavenumber resolution of 0.25 cm^{-1} was used to

collect transmittance spectra at the angle of incidence 30°.

The IR transmittance spectra of the samples under study are in Fig. 1. In this region, the interference effects are present owing to low absorption of IR radiation.

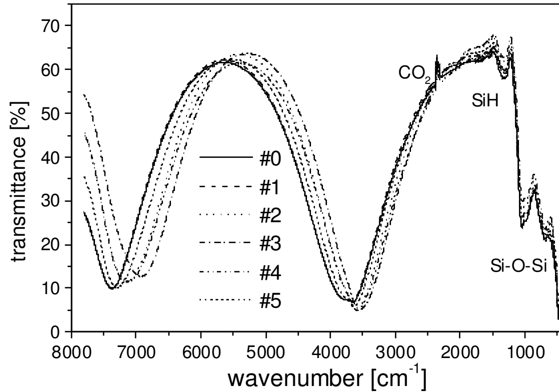

Fig. 1. IR transmittance. Atmospheric CO_2 peak originates from measuring chamber of spectrophotometer. At wavenumbers < 2000 cm^{-1} Si-H and Si-O bonds exhibited.

Horizontal attenuated total reflection Fourier Transform infrared spectroscopy (HATR-FTIR) offers a high sensitivity due to special data acquisition by multipassing and/or multiple reflections at the crystal or the film surface. IR beam enters the crystal with high refractive index and undergoes multiple total internal reflections either at the interface crystal/film or film/substrate depending on the refractive index differences. FTIR absorbance spectra were measured by the HATR accessory with trapezoidal ZnSe crystal with a bevelled edge of 45°.

The absorbance spectra recorded by HATR are in Fig. 2. Owing to the relations of refractive indices at longer wavelengths at interfaces entered by IR radiation (n_{ZnSe} ~ 2.4, n_{glass} ~ 1.5), and n_{Si} ~ 3.5 (Table 2), the total reflections occur at the interface thin film/glass substrate. Therefore, the films is probed by the IR wave and the substrate by the evanescent wave the amplitude A of which decreases exponentially with the distance z from the interface as

$$A = A_0 \exp(-z / d_p) \quad (1)$$

where the penetration depth d_p at the angle of incidence α is defined as

$$d_p = \frac{\lambda}{2\pi\sqrt{\left[\sin^2 \alpha - (n_{glass}/n_{Si})^2\right]}} \quad (2)$$

where λ is the wavelength of the light in silicon. The depth of penetration into the glass substrate at α = 45° is according to Eq. (3) ~ 1.4 μm, thus approximately one third of the wavelength of entering IR wave (at λ = 5 μm). Therefore the advantage of IR measurements probing the whole films in comparison with the Raman measurements probing only a thin layer equal to the penetration depth of the Raman laser beam (for Ar^+ laser beam at 514 nm the depth is only ~ 100 nm in poly-Si) is evident. The depth of penetration into substrate decreases with increasing angle of incidence. Now, let's briefly recall the typical main composition of Corning 1737 aluminosilicate glass – 55% SiO_2, 24 % CaO, 10 % Al_2O_3, 7 % B_2O_3. Fortunately, no Si-H bonds are present in the substrate material probed by the evanescent wave. Si-O bonds coming from the substrate may partly influence the HATR spectra analysis on the oxygen content.

At wavenumbers ~ 2000 cm^{-1}, Si-H absorption bands occur (Fig.2) that are the convolution of predominant monohydride SiH stretching vibrations centered at ~ 2000 cm^{-1} and dihydride SiH_2 at ~ 2090 cm^{-1}. Integral intensities of deconvoluted absorption peaks are proportional to the bonded atom densities. More loose SiH_2 bonds are typical for polycrystalline silicon. Hence, the network reflects not only the crystalline and amorphous volume fractions, but also the monohydride SiH and dihydride SiH_2 environment that definitely influence the mass density of films. The main expected hydride configurations are vacancies and voids. The concept of void-dominated hydride formation at grain boundaries is in Fig.3.

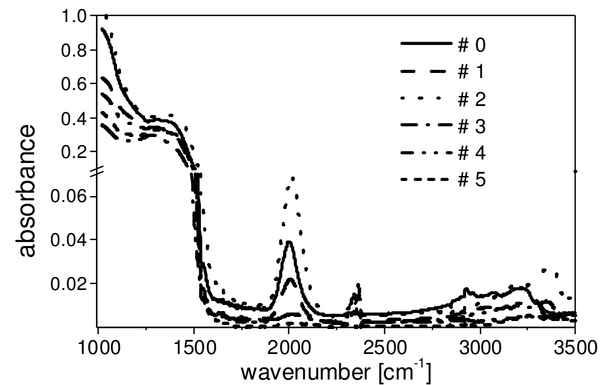

Fig.2. Absorbance spectra (the vertical axis broken to visualise Si-H bands at ~ 2000 cm^{-1}). The region at wavenumbers < 1500 cm^{-1} strongly influenced by the continuum of the substrate.

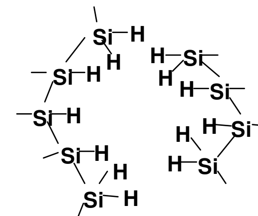

Fig.3. Concept of Si-H bonding at crystalline grain boundaries surrounding voids.

4. RESULTS AND DISCUSSION

In IR region, the photon energy is well below the semiconductor energy gap. Therefore, absorbed

photon energy does not cause the valence-to-conduction band transitions, but displacements of electrons described by the polarizability $p(E)$. The polarizability $p(E)$ together with the spectral complex refractive index $n(E)$ and electron density N enter the well-known Clausius-Mossoti equation [4]

$$\frac{n^2(E)-1}{n^2(E)+2} = p(E)N \qquad (3)$$

The relation (3) enables to determine changes in the mass density of the film with growth-related changes of structure, microstructure and refractive index [5 – 7]. In hydrogenated silicon, the polarizability refers to harmonic dipoles of Si-Si bonds and Si-H bonds oscillators. The presence of hydrogen in Si-H bonding was proved by absorbance bands at ~ 2000 cm^{-1} (Fig.1, 2).

Eq. (3) can be expressed in a more specific form with the polarizability as the sum of individual oscillators (Si-Si bonds in crystalline Si, Si-Si bonds in amorphous Si, Si-H bonds) [6]

$$\frac{n_\infty^{\;2}-1}{n_\infty^{\;2}+2} = \frac{4\pi\rho}{3m_{\mathrm{Si}}}\left(4\xi + \frac{c_{\mathrm{H}}}{1-c_{\mathrm{H}}}(\alpha_3-\xi)\right) \qquad (4)$$

where n_∞ is the refractive index in the long wavelength limit, ρ is the film mass density, $m_{\mathrm{Si}} = 4.664\times10^{-23}$ g is the mass of Si atom, c_{H} is the hydrogen content (Table 1).

Parameter ξ is given by $\xi = [(1-p)\alpha_1 + p\alpha_2]/2$ with p being the amorphous volume fraction. Polarizabilities α_i (i = 1 – 3) correspond to Si-Si bonds in crystalline Si ($\alpha_1 = 1.96\times10^{-24}$ cm^3), Si-Si bonds in amorphous Si ($\alpha_2 = 1.87\times10^{-24}$ cm^3), Si-H bonds ($\alpha_3 = 1.36\times10^{-24}$ cm^3) [6].

Refractive indices n_∞ in the long wavelength limit were determined according to the standard equation for two adjacent interference fringes in the wavenumber region 3500 – 7000 cm^{-1}. The average refractive index in the region between two wavenumbers $\bar{\nu}_m, \bar{\nu}_n$ (Fig.1) is given by $n_\infty = \dfrac{1}{2d(\bar{\nu}_n - \bar{\nu}_m)}$. When calculating n_∞, the spectral dependence $n(\bar{\nu})$ in the region far from the absorption edge was supposed to be negligible. The correction for the angle of incidence at transmission measurements was involved. The values obtained for n_∞ (Table 2) apparently decrease with increasing dilution of SiH_4 plasma from which the sample were deposited.

From Eq. (4), the film mass density ρ_1 was calculated first for the amorphous volume fraction determined from Raman spectra neglecting the void volume fraction. The results are in Table 2.

The values ρ_1 were then corrected considering void volume fractions that were deduced from effective media approximation applied upon refractive indices n_∞. According to the various theories of effective media approximations (EMA) [8 – 10], a mixture of different materials can be considered as a homogenous medium having an effective refractive index that can be obtained from the refractive indices and the volume fractions of individual components.

Tab. 2. Refractive index n_∞ in the long wavelength limit, amorphous volume fraction p_a according Raman spectra, mass density ρ_1 calculated without considering voids.

Sample	Dilution	p_a [%]	n_∞	ρ_1 [g/cm^{-3}]
# 0	0	100	3.805	2.378
# 1	10	100	3.633	2.357
# 2	20	100	3.601	2.346
# 3	30	39	3.508	2.280
# 4	40	27	3.520	2.271
# 5	50	18	3.425	2.235

According to Bruggemans's EMA (BEMA) [8] dealing with the complexity of mixed-phase materials, the complex dielectric function ε of a composite film is given by the equation

$$\sum_i p_i \frac{\varepsilon_i - \varepsilon_{eff}}{\varepsilon_i + 2\varepsilon_{eff}} = 0 \qquad (5)$$

where ε_{eff} is the effective dielectric function, the sum goes over i constituents with dielectric functions ε_i and volume fractions p_i, while $\sum_i p_i = 1$.

The method performs well with two constituents. The case of more than two constituents is associated with either the selection of the proper solution from multiple inverse of Eq. (5) or with some prior physically meaningful knowledge of the material.

Regarding that in the non-absorbing spectral region is $n = \sqrt{\varepsilon}$, $n_{eff} = n_\infty$ and three constituents are of volume fractions p_c (crystalline Si), p_a,(a-Si:H) and p_v (voids filled with air), Eq. (5) can be written as

$$p_a \frac{n^2_{\mathrm{a-Si:H}} - n^2_\infty}{n^2_{\mathrm{a-Si:H}} + 2n^2_\infty} + p_c \frac{n^2_{\mathrm{c}} - n^2_\infty}{n^2_{\mathrm{c}} + 2n^2_\infty} + \\ + p_v \frac{1-n^2_\infty}{1+2n^2_\infty} = 0 \qquad (6)$$

For refractive indices In Eq. (6), the following values $n_{\mathrm{a-Si:H}}$ = 3.805 (sample #0), n_{c} = 3.42 [6], n_{void} = 1 were applied.

As the prior knowledge the degree of crystallinity (Table 1) expressing the ratio of amorphous to crystalline volume fractions (determined from Raman spectra scattering [2]) was used. The results for volume fractions p_c, p_a, p_v are in Table 3. As the fraction of crystalline part rises with increasing dilution, the amorphous fraction obviously decreases generating increased fraction of

voids. This result coheres with the data for mass density ρ_2 also seen in Table 3 that were calculated according to Eq. (4) for amorphous volume fraction from Table 3.

The mass density ρ_2 and n_∞ are plotted in Fig. 4 versus hydrogen content. Two quasi-linear regions can be seen in both plots. The first region belonging to hydrogen content < 5 % corresponds to polycrystalline Si deposited at higher dilutions. We speculate that small hydrogen content and mass density origin from void-dominated network formation. On the contrary, the amorphous regime in Fig. 4 at c_H > 10 % corresponds to denser films with higher refractive index and the vacancy-dominated mechanism of network formation. The results are in contrary to the mass density evolution with hydrogen content reported in [7] for expanding thermal plasma deposited films.

Tab. 3. The mass density ρ_2 examined considering void volume fraction according BEMA , p_c (p_a, p_v) – the crystalline (amorphous, void) volume fractions, respectively.

Sample	p_c [%]	p_a [%]	p_v [%]	ρ_2 [g/cm^{-3}]
# 0	0	100	0	2.378
# 1	0	93.4	6.6	2.350
# 2	0	92.2	7.8	2.338
# 3	58.2	36.0	5.8	2.277
# 4	68.2	25.0	6.8	2.267
# 5	72.0	16.0	12.0	2.233

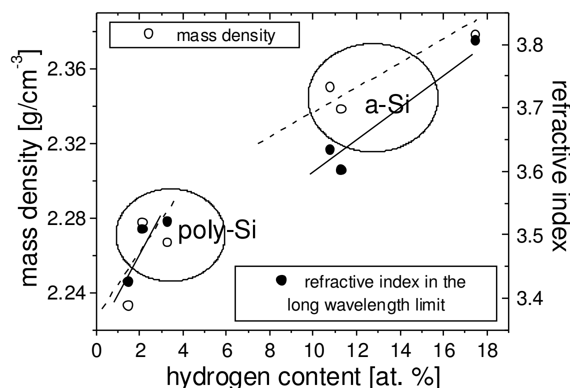

Fig.4. The mass density and the refractive index in the long wavelength limit versus the hydrogen content in atomic percent.Small circles refer to the values determined from IR experiments,the lines correspond to two indicated regions in the Si network formation.

5. CONCLUSION

A more detailed interpretation of IR spectra was used to obtain better insight into the mutual relations between dilution as a growth parameter and the refractive index, the hydrogen content and the mass density of material. Analysis of FTIR spectra shows corresponding decrease of hydrogen content, refractive index in the long wavelength limit and the mass density of silicon thin film deposited by PECVD under increasing dilution of silane plasma and increasing order in Si network.

According to the results, refractive index in the long wavelength limit not only belongs to important optical properties of material, but is also related to the structure and microstructure. Especially hydride configurations in vacancies and voids seem plausible to induce observed changes.

Acknowledgement

This work was supported in part by the Slovak Grant Agency under grant No.2/4105/04. Dr V. Nádaždy at the Institute of Physics, Slovak Academy of Sciences, Bratislava, Slovakia, is acknowledged for the sample preparation.

REFERENCES

[1] V. Nádaždy, M. Zeman: *Phys. Rev. B 69 (2004) 165213.*
[2] J. Müllerová, S. Jurečka, P. Šutta: *Acta Phys. Slovaca 55 (2005) 351.*
[3] J. Müllerová, S. Jurečka, P. Šutta: *Solar Energy (2006), in press.*
[4] C. Kittel: *Introduction to Solid State Physics. New York: Wiley, 5 ed., 1976.*
[5] Z. Remeš, M. Vaněček, A.H. Mahan, R.S. Crandall: *Phys. Rev. B56 (1997) 12710.*
[6] Z. Remeš, M. Vaněček, P. Torres, U. Kroll, AH. Mahan, R.S. Crandall: *J. Non-Cryst. Solids 227-230 (1998) 876.*
[7] A.H.M. Smets, W.M.M. Kessels, M.C.M. van den Sanden: *Appl. Phys. Lett.82 (2003) 1547.*
[8] D. A. G. Bruggeman: *Ann. Phys. 24 (1935) 636.*
[9] H.C. Lee, S.I. Lee, H. Lee, S.H. Choi, J.I. Ryu, J. Jang: *J. Korean Phys. Society, 39 (2001), S30*
[10] K. Mui, D.K. Basa, F.W. Smith: *Phys. Rev. B 35 (1987) 8089.*